IEEE Transactions on Nuclear Science, Vol.NS-24, No.3, June 1977

DESIGN CONCEPT FOR A 100 GeV e^+-e^- STORAGE RING

R. Billinge, P. Bramham, H.F. Hoffmann, A.M. Hutton, K. Johnsen,
E. Jones, E. Keil, B. Richter*, W. Schnell, A. Verdier, E.J.N. Wilson
CERN
Geneva, Switzerland

1. Introduction and Summary

A conceptual design of a 100 GeV e^+-e^- storage ring (LEP) being studied at CERN and some of the problems encountered are presented. The 20 GeV fast-cycling injector synchrotron is studied at the Rutherford Laboratory.[1] To obtain a luminosity $L = 1 \times 10^{32}$ cm^{-2} s^{-1} at 100 GeV, the product of bending radius ρ and the RF power P_B delivered to both beams must be $P_B \rho = 136$ GWm, assuming optimum coupling, a maximum permissible beam-beam tune shift $\Delta Q = 0.06$, and a vertical amplitude function $\beta_y^* = 0.01$ m at the crossings. The bending radius $\rho = 6.1$ km was obtained by cost optimisation.[2]

2. Lattice

The lattice shown in Fig. 1 gives the correct beam size at 100 GeV.[3] Starting from a crossing point, the magnet arrangement contains the low-β insertion, the RF straight section, both with zero dispersion, a wiggler insert with enlarged dispersion, a dispersion suppressor and normal cells up to the centre of the arc, a symmetry point. The dispersion is manipulated by leaving out or modifying bending magnets; the quadrupole arrangement and hence the behaviour of the amplitude functions are regular except for four quadrupoles either side of the intersections. The LEP parameters are summarized in Table I. The free space near the crossing points, ± 10 m, is adequate for most experiments.[4] At reduced luminosity, more space could be provided. The normal lattice cells have separated functions and a phase advance of $\approx \pi/3$, a favourable value for chromaticity correction.[5] The number of bunches is determined by beam loading of the RF system (cf. section 3). Since there are only eight crossing regions, the beams must be separated by electrostatic plates in 56 places. A lower limit for β_y^* is given by the beam-beam bremsstrahlung lifetime. In a fully coupled machine β_x^* should be equal to β_y^*. The value taken is a compromise between this requirement and the horizontal chromaticity.

Table I - LEP parameters at 100 GeV

Luminosity	1.117×10^{32} cm^{-2} s^{-1}
Beam-beam tune shift	0.06
Number of bunches	32
Circulating current	15.34 mA
Hor. ampl.fct. at crossing β_x^*	0.625 m
Vert. ampl.fct. at crossing β_y^*	0.1 m
Hor. rms beam radius at crossing	93.6 µm
Vert. rms beam radius at crossing	37.4 µm
Beam-beam bremsstrahlung lifetime	13.9 h
Synchrotron radiation loss/turn	1.44 GeV
Higher mode loss/turn	120 MeV
Peak RF voltage/turn	1.72 GV
Active length of RF structure	2469 m
RF generator power	109 MW

The most satisfactory chromaticity correction scheme found so far involves six families of sextupoles and results in a tune variation $\Delta Q = 0.067$ for a momentum width of $\Delta p/p = \pm 0.8\%$. The stability of betatron oscillations with finite amplitudes has been investigated using the tracking programs LIMATRA [6] and PATRICIA [7]; for the 50 GeV configuration, which has the largest amplitudes, amplitudes up to seven standard deviations in both planes simultaneously are stable.

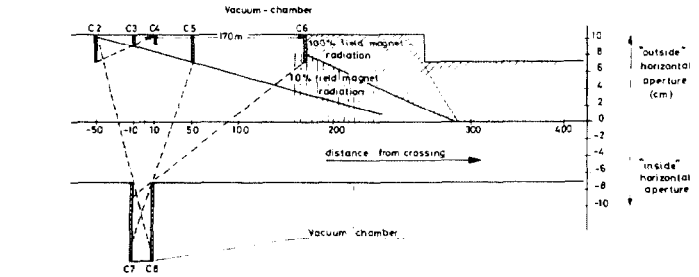

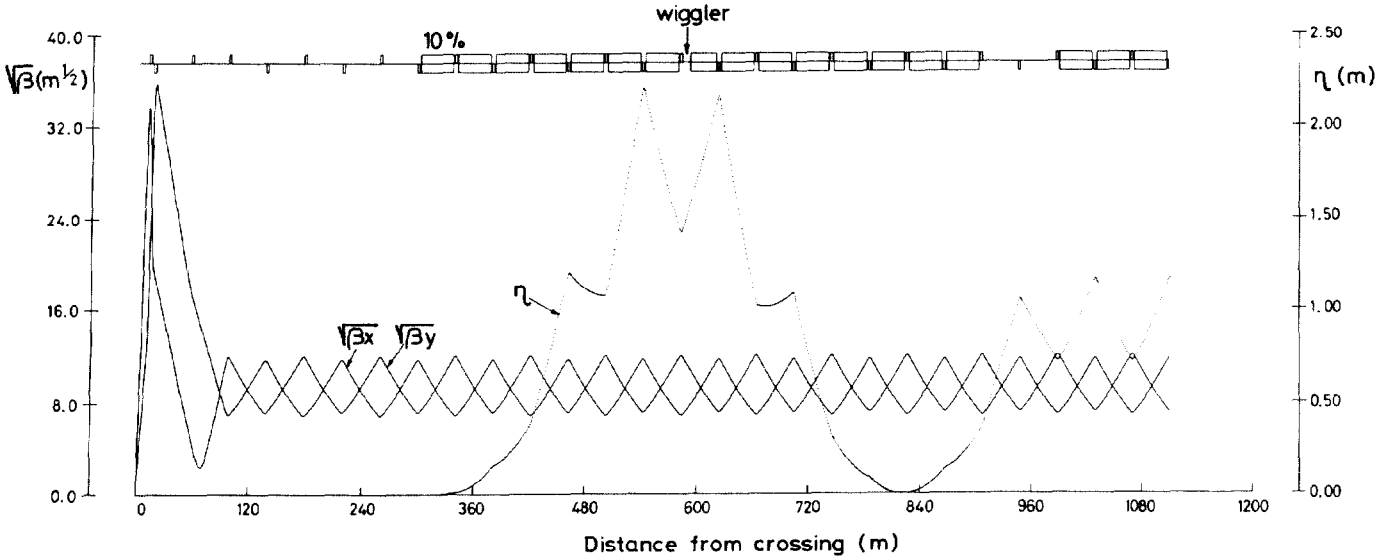

Fig. 1 - Lattice and collimator layout and orbit functions near crossings.

*) permanent address: SLAC, Stanford, California, U.S.A.

Closed orbit distortions cause coupling and vertical dispersion. Full coupling, i.e. equal horizontal and vertical emittances are expected. The vertical dispersion causes a loss of luminosity, unless it is corrected in the crossing points,[8] and a change in the damping partition numbers, which has been investigated using the PETROS program.[9] The closed orbit must be corrected to a standard deviation of a few millimetres, if antidamping in one of the degrees of freedom is to be avoided.

The luminosity and beam parameter variation shown in Fig. 2 is obtained by wiggler magnets.[10] The wiggler magnets affect both the energy spread which should be kept as small as possible and the emittance. Placing them at a high dispersion zone enhances their effect on the emittance, and permits L to be kept constant from 50 to 100 GeV, and the emittance constant from 20 to 50 GeV ($L \propto E^2$). With 64 m of wigglers the maximum field is only 0.416 T. A detailed analysis of the synchrotron radiation emitted in the wiggler magnets shows that individual magnets must be short (2 m has been adopted) to keep the maximum surface power density below 100 W/cm^2. The maximum critical energy is 1.3 MeV, and a significant fraction of the photons are above the threshold for γ-n reactions. About 4×10^9 neutrons/s are produced per metre of wiggler magnet, spread out over about 120 m of circumference.

3. RF System and Beam Loading

The main RF parameters are shown in Table I. Frequencies from 200 to 500 MHz have been considered. A high frequency is preferred to limit the size of the RF cavities, the power dissipated per unit length of structure, and the cost of RF power sources. The number of synchrotron oscillation per revolution, Q_S, which is of some importance for betatron synchrotron coupling resonances and should be less than about 0.1, favours a lower frequency. None of these arguments is very strong and hence the average between the two limits, 350 MHzm, has been adopted.

The power which the RF system must supply to the beams P_B is fixed by the lattice and performance, while the energy U extracted by a bunch on a single passage is inversely proportional to the number of bunches K_b. An upper limit for the ratio η between U and the stored energy W in the cavity is given by [11]

$$\eta = U/W = 2\pi\, h\, P_B/K_b\, Q\, P_\ell < B^{-1} \sin^2 \phi \qquad (1)$$

Here, h is the harmonic number, Q the quality factor of the cavity, P_ℓ the power lost in the cavity walls, and ϕ the stable phase angle. The beam loading enhancement factor $B > 1$ is the ratio of the energy radiated into all modes to that radiated into the lowest mode of an unexcited cavity. It depends only on the bunch and cavity geometry. For $K_b = 32$, one finds $\eta = 0.349$, which, for $\sin \phi = 0.927$ does not violate (1) for $B < 2.46$, a reasonable figure.

Accelerating cavities follow the PETRA design [12] with all relevant dimensions scaled from 500 to 350 MHz. Each cavity consists of five cells operated in π mode. Coupling between cells is by slots in the discs. RF power is fed into the central cell of each cavity by means of a coupling loop. The second and fourth cells have motor-driven tuning plungers. RF power is supplied by large klystron amplifiers each feeding four cavities. Each klystron is located with its circulator, high-voltage supply, driver, and associated equipment in an annex alongside the tunnel. RF power is carried by rectangular waveguide into the tunnel, and divided between cavities by hybrids used as two-way splitters. Path lengths to all cavities are the same.

4. Magnet and Vacuum System

The dipole magnetic field is 0.05437 T at 100 GeV, and 0.01087 T at injection. Such low fields virtually exclude the distributed type of sputter-ion pump commonly employed in electron storage rings. Also the need to avoid excessive higher mode losses at discontinuities in the vacuum chamber implies a cross-section

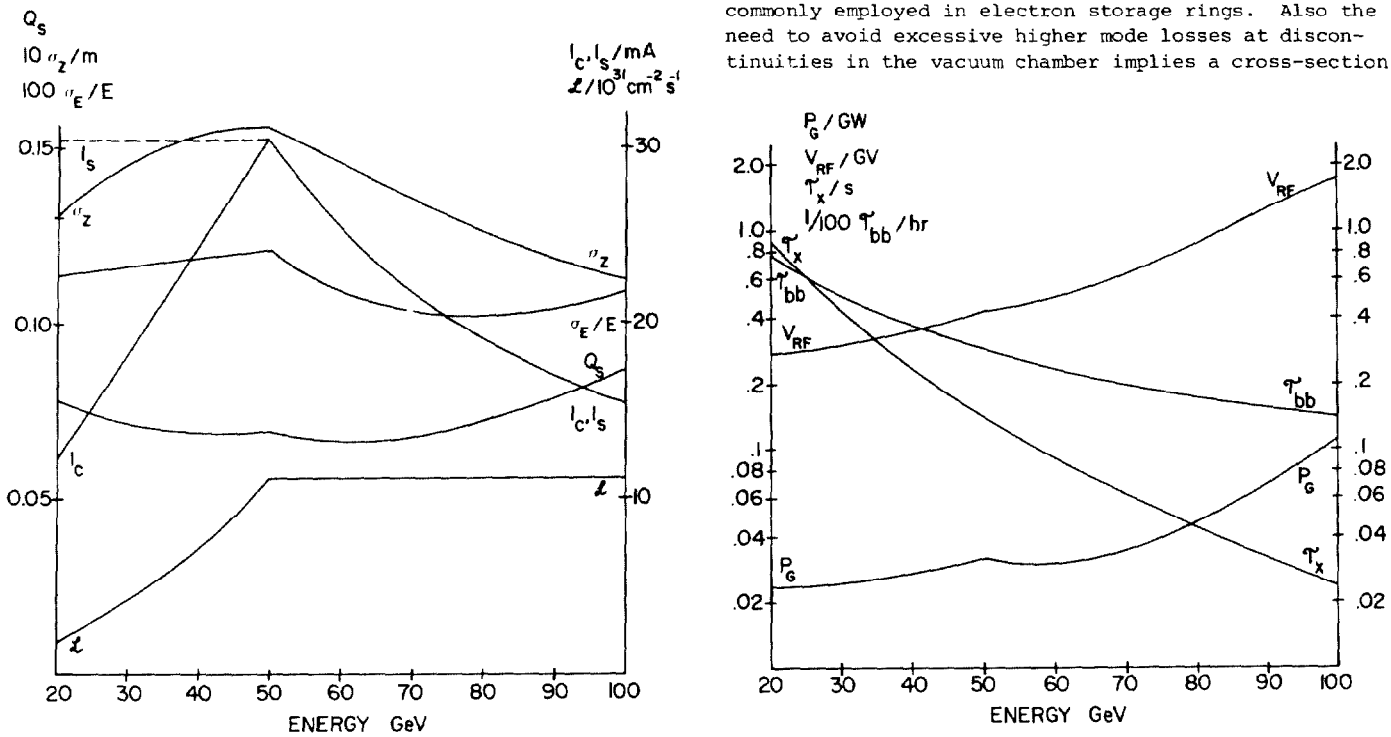

Fig. 2 - Variation with energy of stored current I_S, collision current I_C, energy spread σ_E/E, bunch length σ_Z, damping time τ_x, bremsstrahlung time τ_{bb}, RF voltage V_{RF}, RF generator power P_G.

which is as constant as possible around the ring. In the focusing structure proposed, this leads to a roughly circular aperture requirement. The minimum apertures shown in Table I together with the pumping speed required indicate a beam pipe of 20 cm nominal diameter. In this way, lumped pumping at each quadrupole will be sufficient to maintain a vacuum of 10^{-8} Torr at the middle of the 35 m long bending magnets, for a linear desorption coefficient due to both thermal outgassing and synchrotron radiation of $\sim 5 \times 10^{-8}$ Torr $\ell\ s^{-1}\ m^{-1}$.

In conventional H or window-frame magnets, the field shape is determined almost entirely by the steel poles. The permeability of magnet steel which can be produced in large quantities and at low cost, is both very low and varies with field, typically from $\mu = 200$ at 0.01 T to $\mu = 2000$ at 0.05 T. To minimize distortion of the field shape due to these effects and consistent with the large circular aperture required, the dipole consists of shaped Al conductors, surrounded by a steel outer shell shaped to give uniform flux density in the steel. The quadrupoles and sextupoles are of conventional design and have relatively high field at their poletips, so that integrated ion pumps may be envisaged there. The cross-section of the magnets and common vacuum chamber is illustrated in Fig. 3. The small circular holes are cooling channels and the large rectangular holes at top and bottom of the vacuum chamber are to contain sputter-ion pump elements. Two elements in a 2.5 m long quadrupole provide a minimum pumping speed near injection of 600 $\ell\ s^{-1}$.

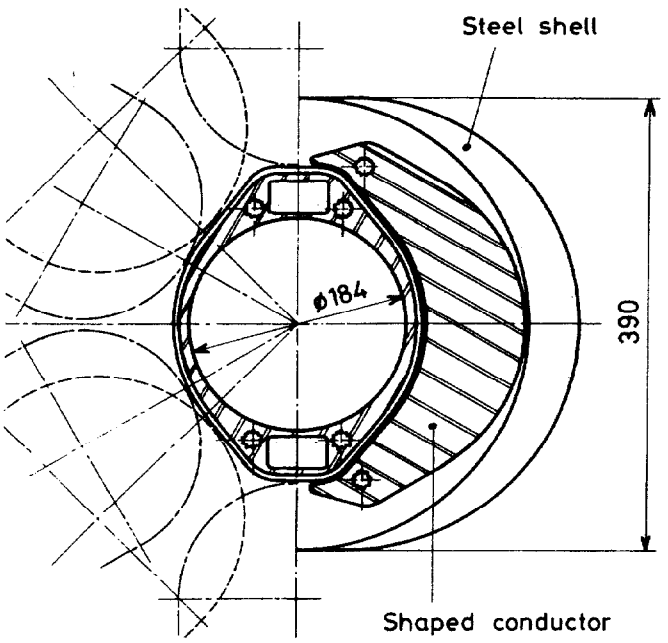

Fig. 3 - Cross-section of magnets and vacuum chamber.

To avoid costly bus-bar systems, the dipoles and quadrupoles are connected and powered in series for the whole ring and this also improves tracking. With this system of magnet excitation, it is possible to maintain a low total voltage and use simple minerally insulated magnet coils.

When the beam is circulating, the quadrupoles and dipoles are powered and hence the pumps installed in the quadrupoles help handle the gas desorbed by synchrotron radiation. The sextupoles are powered independently and the pumping elements of about 60 $\ell\ s^{-1}$ installed therein can be used as holding pumps when the machine is switched off. In this way, they have to take care only of thermally desorbed gas which has been estimated at some 10% of the synchrotron radiation induced gas load. All these estimates are based on extrapolations from SPEAR data.[13] It is implicit in this design that during the first months of operation the Al alloy vacuum chamber will have to be cleaned intensively by "beam scrubbing" with the electrons produced in the interaction between the synchrotron radiation and the chamber wall.

Because the interaction regions are shielded from synchrotron radiation, their vacuum system is not expected to present any particular problems. However, the synchrotron shields themselves and the wiggler magnet regions present special vacuum problems.

5. Synchrotron Radiation and Background

The detectors in the crossing regions are shielded from synchrotron radiation generated in the arcs by a bending magnet with 10% of the normal field, and a system of collimators,[14] shown in Fig. 1. If the beams are located in the intersection region vacuum chamber such that the distance to the outside wall is 9 cm, and 15 cm to the inside, the photons generated in the low-field magnet must be scattered at least twice before they can reach the detector, while photons generated in the quadrupoles of the straight lattice must be emitted by electrons with a divergence $> 10\ \sigma$ to reach the detector by scattering; those emitted at smaller angles pass through the interaction regions.

A second source of background is the collision between the e^+ or e^- bunches and the synchrotron radiation bunch accompanying the opposite beam. Most of the Compton-scattered electrons and photons occur at very small angles and will be invisible to experiments. The pair-produced electrons appear at larger angles at a rate < 20 kHz. These processes must be taken into account in the design of $\gamma\gamma$-experiments.

6. Conclusions

The study of LEP has not yet revealed any unsurmountable technical problems, apart from those associated with its size and number of components. Tolerances on most components are much tighter than in existing e^+-e^- storage rings, or in PEP and PETRA. Studies are continuing on whether these tolerances can be eased by a different approach to the lattice design.

References

1. J.R.J. Bennett et al.; this Conference (M-14)
2. B. Richter; Nucl. Instr. Methods 136 47 (1976)
3. J. Rees and B. Richter; SLAC Report PEP-69 (1973)
4. L. Camilleri et al.; CERN 76-18
5. B. Autin; CERN Int. rep. ISR-LTD/76-37
6. G. von Holtey; CERN Int. rep. Lab.II-DI-PA/Int.75-3
7. H. Wiedemann; SLAC Report PEP-220 (1976)
8. R. W. Chasman and M. Month; BNL 50529 (1976)
9. K. Steffen and J. Kewisch; private communication
10. A. Hutton; CERN Int. rep. ISR-LTD/76-20
11. E. Keil et al; CERN Int. rep. ISR-LTD/76-22
12. PETRA Proposal, DESY (1974)
13. D. Bostic et al.; IEEE Trans. Nucl. Sci. NS-22, No. 3, 1540 (1975)
14. H.F. Hoffmann and B.H. Wiik; in ref. 4, p. 203